Electric-field-controlled electron relaxation in lateral double quantum dots embedded in a suspended slab

Y. Y. Liao, D. S. Chuu, and S. R. Jian

Citation: Journal of Applied Physics **104**, 104315 (2008); doi: 10.1063/1.3009960
View online: http://dx.doi.org/10.1063/1.3009960
View Table of Contents: http://scitation.aip.org/content/aip/journal/jap/104/10?ver=pdfcov
Published by the AIP Publishing

Electric-field-controlled electron relaxation in lateral double quantum dots embedded in a suspended slab

Y. Y. Liao,[2,a] D. S. Chuu,[1] and S. R. Jian[3]
[1]*Department of Electrophysics, National Chiao-Tung University, Hsinchu 300, Taiwan*
[2]*Department of Applied Physics, National University of Kaohsiung, Kaohsiung 811, Taiwan*
[3]*Department of Materials Science and Engineering, I-Shou University, Kaohsiung 840, Taiwan*

(Received 16 January 2008; accepted 18 September 2008; published online 21 November 2008)

This study investigates phonon-induced electron relaxation in a lateral double quantum dot that is embedded in a suspended slab. Exact calculations are made in electric fields. The dependence of the relaxation rate on the parameters of the dots and the slabs is analyzed. Numerical results indicate that the relaxation rate depends strongly on the phonon character of the slab. Unlike in the bulk environment, phonon-subband quantization clearly influences the behavior. In particular, the relaxation rate can be greatly suppressed or enhanced by tuning the electric fields. This fact may be useful in manipulating the relaxation rate in lateral double quantum dots. © *2008 American Institute of Physics*. [DOI: 10.1063/1.3009960]

I. INTRODUCTION

The recent fabrication of quantum dots (QDs) in nanometer dimension has led to much theoretical and experimental research interests in the QD systems.[1,2] Gate-defined QDs are laterally fabricated from a two-dimensional electron gas in a GaAs/AlGaAs heterostructure.[3,4] Lateral QDs are further grown by self-assembly techniques.[5,6] QDs are regarded as being crucial to solid-state quantum devices, providing a significant advantage of controllability via external voltages. Their atomlike properties and their highly flexible size and shape make them ideal for numerous potential applications.[7–11]

QDs are solid-state structures embedded in the surrounding macroscopic crystal. Electrons in QDs always interact with the lattice according to its degrees of freedom. Hence, phonon-induced relaxation can occur, preventing the electron from remaining for long in a quantum state without loss. In lateral or vertical QDs, the few meV of separation between the energy levels is less than the optical phonon energy, and so electron relaxation is dominated by acoustic phonon scattering. Correspondingly, the relaxation times from excited states are limited to the order of nanoseconds in GaAs-based QDs.[12] Many theoretical studies of electron relaxation in single and double QDs have been performed.[13–16] Electron-phonon scattering can be effectively suppressed using various mechanisms to improve the performance of QD devices.[17–21] The manipulation and understanding of the electron relaxation in QDs are therefore of great importance in the design and the operation of the quantum devices.

Since the features of QDs are controllable, external influences on electron relaxation in QDs become an important topic.[16–20] Even though considerable effort has been made to analyze bulk systems, the relaxation of a lateral double QD in a confined structure has received little attention. Unlike in the bulk, the confined structure enables the phonon density of states to be controlled: the electron-phonon interaction can be tailored by altering the dimensions. Intuitively, electron-phonon scattering is expected to reveal some interesting properties of confined structures. This work elucidates electron relaxation in a lateral double QD embedded in a suspended slab. The system is subjected to an in-plane electric field in the interdot direction. Exact diagonalization is used in numerical calculations to show that the structural parameters and electric field strongly affect the relaxation rate. In particular, the phonon characteristics of the slab determine this rate. The relaxation rate can be varied by several orders of magnitude by tuning the field strength.

II. MODEL AND METHOD

Figure 1 depicts a GaAs double dot embedded inside a suspended slab with two boundaries at $z=\pm L/2$. The structure was realized with the help of advanced nanotechnology.[22,23] The Hamiltonian for an electron in a double QD subjected to an in-plane electric field can be written as

$$H=\frac{\mathbf{p}^2}{2m^*}+V_c(\mathbf{r}_\parallel)+V_w(z)+V_{\mathrm{ext}}(\mathbf{r}_\parallel), \tag{1}$$

where $\mathbf{p}=-i\hbar\nabla$, m^* is the electron effective mass and V_c is the xy-plane confinement potential,

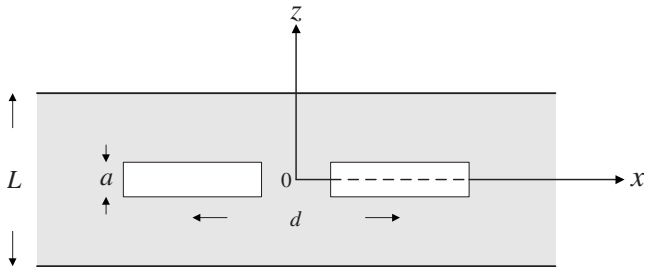

FIG. 1. Schematic view of a double QD embedded in a suspended semiconductor slab with a width of L. The vertical width of the dot is a and the interdot distance is d. The double dot is located in the center of the slab. Here we simply illustrate the dots with blocks.

[a]Electronic address: yyliao@nuk.edu.tw.

$$V_c = \frac{1}{2}m^*\omega_0^2 \min\left[\left(x-\frac{d}{2}\right)^2 + y^2, \left(x+\frac{d}{2}\right)^2 + y^2\right], \quad (2)$$

with $\mathbf{r}_\parallel=(x,y)$, interdot distance is d, and confinement frequency is ω_0. For vertical confinement, V_w is given by $V_0\Theta(|z|-a/2)$, where a is the vertical width of the QD. The potential is taken as an infinite quantum well ($V_0\to\infty$). Because its confinement is much stronger than that in the xy-plane, a relevant wave function is $\varphi(z)=\sqrt{2/a}\cos(\pi z/a)$. Analysis using the model indicates that only the x component of the electric field is relevant. Accordingly, the interaction between an electron and an electric field in the x direction can be expressed as

$$V_{\text{ext}} = -eFx, \quad (3)$$

with the electron charge as e and the field strength as F.

A numerical solution to the Hamiltonian of electron can be obtained by expanding the wave function in a basis set with a large number of eigenstates of the single-dot wave functions,

$$\Psi(r_\parallel,\theta,z) = \sum_{m,l} c_{ml}\psi_{ml}(r_\parallel,\theta)\varphi(z). \quad (4)$$

Here, the basis wave functions ψ_{ml} are the well-known Fock–Darwin states,[24]

$$\psi_{ml}(\rho,\theta) = \sqrt{\frac{m!}{\pi\alpha^2(m+|l|)!}}\rho^{|l|}e^{-\rho^2/2}L_m^{|l|}(\rho^2)e^{il\theta}, \quad (5)$$

and their corresponding electron energy levels are

$$E_{ml} = \hbar\omega_0(2m+|l|+1), \quad (6)$$

where $L_m^{|l|}(\rho)$ is an associated Laguerre polynomial and $\rho=r_\parallel/\alpha$ is a scaled radius with effective QD lateral length $\alpha=\sqrt{\hbar/m^*\omega_0}$. In the equations m $(=0,1,2,\ldots)$ and l $(=0,\pm1,\pm2,\ldots)$ are quantum numbers. Exact diagonalization of the electron Hamiltonian allows the corresponding eigenvalues and coefficients to be obtained numerically. Notably, the chosen basic set $\{\psi_{ml}\}$ provides stable convergence for Eq. (1) with increasing m. The method and basis are analogous to those used in a study of a lateral double QD system.[25] As an example, the error for the lowest five energy levels is lower than 10^{-7} for $m_{\max}\sim 20$, causing convergence in the electron relaxation rate to within 1%.

The electron relaxation rates due to acoustic-phonon scattering between the two lowest states are calculated using the Fermi golden rule,[26]

$$\Gamma = \frac{2\pi}{\hbar}\sum_{\mathbf{q}_\parallel,n,\sigma}|\langle f|M_n^\sigma e^{i\mathbf{q}_\parallel\cdot\mathbf{r}_\parallel}|i\rangle|^2(n_{\mathbf{q}_\parallel n}^\sigma+1)\delta(\Delta E-\hbar\omega_{\mathbf{q}_\parallel n}^\sigma), \quad (7)$$

where σ is the phonon mode and n is the branch. ΔE denotes the energy difference between the first excited state $|i\rangle$ and the ground state $|f\rangle$. $n_{\mathbf{q}_\parallel n}^\sigma$ represents the Bose distribution with in-plane wave vector $\mathbf{q}_\parallel=(q_x,q_y)$. To evaluate the phonon frequency $\omega_{\mathbf{q}_\parallel n}^\sigma$, the elastic properties of the slab are assumed to be isotropic, based on the elastic continuum model. Small elastic vibrations of the slab are defined by the displacement vector $\mathbf{u}(\mathbf{r})$. Under the isotropic elastic continuum approximation, the equation for the displacement vector is[27]

$$\frac{\partial^2\mathbf{u}}{\partial t^2} = c_t^2\nabla^2\mathbf{u} + (c_l^2-c_t^2)\nabla(\nabla\cdot\mathbf{u}), \quad (8)$$

where c_l and c_t are the speeds of longitudinal and transverse acoustic waves, respectively. The confined phonon model can be solved by matching the boundary conditions. The three confined acoustic modes are shear waves, dilatational waves, and flexural waves. An important feature of the confined modes is the quantization in the z direction; the z component of the wave vector q_z, is directly related to the width of the slab. For shear waves, they are purely transverse waves and their dispersion relation (superscripts omitted) is $\omega_{\mathbf{q}_\parallel n}=c_t\sqrt{q_\parallel^2+q_{z,n}^2}$, where $q_{z,n}$ depends on $n\pi/L$. Here, q_z is labeled by an additional index n. Following Ref. 28, the electron-phonon interaction is $H_{\text{ep}}=E_a\nabla\cdot\mathbf{u}(\mathbf{r})$ with the deformation potential constant E_a. The shear waves can be neglected because they do not interact with electrons through the deformation potential ($\nabla\cdot\mathbf{u}=0$). Additionally, the phonon dispersion relations for the other waves are given by[28]

$$\omega_{\mathbf{q}_\parallel n} = c_l\sqrt{q_\parallel^2+q_{l,n}^2} = c_t\sqrt{q_\parallel^2+q_{t,n}^2}, \quad (9)$$

where $q_{l,n}$ and $q_{t,n}$ are determined from equations

$$\frac{\tan q_{t,n}L/2}{\tan q_{l,n}L/2} = -\frac{4q_\parallel^2 q_{l,n}q_{t,n}}{(q_\parallel^2-q_{t,n}^2)^2}, \quad (10)$$

for the dilatational waves, and

$$\frac{\tan q_{l,n}L/2}{\tan q_{t,n}L/2} = -\frac{4q_\parallel^2 q_{l,n}q_{t,n}}{(q_\parallel^2-q_{t,n}^2)^2}, \quad (11)$$

for the flexural waves. Correspondingly, the function M_n^i describes the coupling strength of the electron that interacts with the dilatational waves,

$$M_n^d(\mathbf{q}_\parallel,z) = F_n^d\sqrt{\frac{\hbar E_a^2}{2A\rho\omega_{\mathbf{q}_\parallel,n}}}(q_{t,n}^2-q_\parallel^2) \times(q_{l,n}^2+q_\parallel^2)\sin\left(\frac{q_{t,n}L}{2}\right)\cos(q_{l,n}z), \quad (12)$$

and with the flexural waves,

$$M_n^f(\mathbf{q}_\parallel,z) = F_n^f\sqrt{\frac{\hbar E_a^2}{2A\rho\omega_{\mathbf{q}_\parallel n}}}(q_{t,n}^2-q_\parallel^2) \times(q_{l,n}^2+q_\parallel^2)\cos\left(\frac{q_{t,n}L}{2}\right)\sin(q_{l,n}z), \quad (13)$$

where F_n^d (F_n^f) is the normalization constant, A is the area of the slab, and ρ is the mass density.

The importance of the piezoelectric potential can be compared with that of the deformation potential. The ratio of the piezoelectric potential strength to the deformation potential strength depends on $(ee_{14}/E_aq)^2$, where e_{14} is the piezoelectric constant, and q is the wave vector.[29,30] In bulk GaAs systems, piezoelectric interaction typically dominates for long-wavelength acoustic phonons.[31,32] For the slabs, however, confinement yields a lower bound for q, which is equal to π/L, because of the q_z quantization.[28] This cuts off phonons with low momenta that determine the strength of

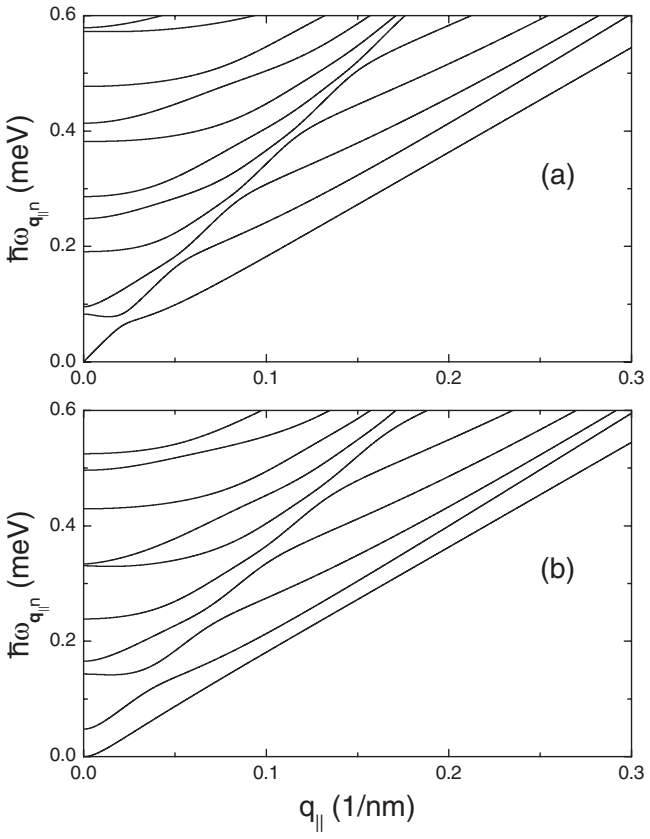

FIG. 2. Dispersion relations $\hbar\omega_{\mathbf{q}_\parallel n}$ for (a) dilatational and (b) flexural waves with $L=130$ nm.

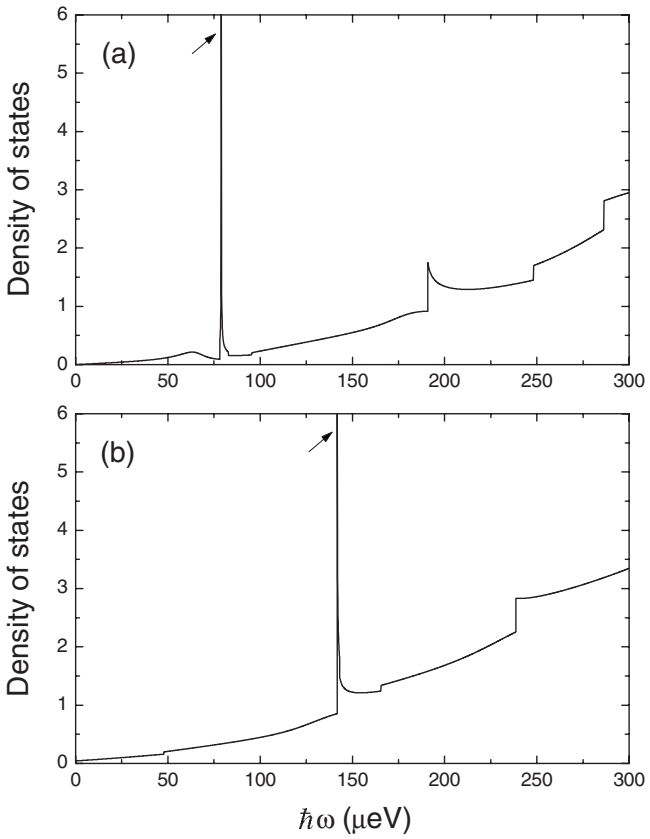

FIG. 3. Density of states (arbitrary units) as a function of energy $\hbar\omega$ for (a) dilatational and (b) flexural waves. The arrows are used to indicate the van Hove singularities.

the piezoelectric electron-phonon coupling. Accordingly, deformation potential can be argued to be the main determinant of the confined phonon geometries.[28,33] The numerical results for electron relaxation in a GaAs double QD are presented below. The material parameters are taken from Ref. 29. To explicate the main feature of one-phonon processes, the calculation assumes a zero temperature such that the phonon absorption can be neglected. Unless otherwise specified, all calculations are performed for a slab width $L=130$ nm, a lateral confinement potential $\hbar\omega_0=1$ meV, an interdot distance $d=150$ nm, and a vertical width $a=8$ nm.

III. RESULTS AND DISCUSSION

Equations (9)–(11) yield numerical results for the dispersion relations. Figures 2(a) and 2(b) show the complex character of the spectra of dilatational and flexural waves. Confined phonons are evidently quantized in subbands. For most branches, the energy increases with the in-plane component $q_\parallel$. In particular, the curve exhibits a remarkable behavior. As presented in Fig. 2, the second dilatational mode and the third flexural mode decrease to a minimum and then increase in the small $q_\parallel$ regime, reflecting the fact that the phonon group velocity is zero at some value $q_\parallel$.

The phonon properties of the slab are now considered. The phonon density of states is given by

$$\rho(\omega)=\sum_{\mathbf{q}_\parallel,n}\delta(\omega-\omega_{\mathbf{q}_\parallel n}). \tag{14}$$

Based on the dispersion relations, Fig. 3 presents the density of states for dilatational and flexural modes. The curves are not congruous because the parameters $(q_\parallel,q_{l,n},q_{t,n})$ of the dilatational and flexural waves independently satisfy the dispersion relations. As the energy increases, phonon-subband quantization produces a staircaselike curve. Each step corresponds to the onset of a new subband, which starts to contribute to the density of states. Specifically, a fine but very large density of states (arrow) is observed. It originates from the van Hove singularity, which corresponds to a minimum in the dispersion relation, as shown in Fig. 2.[28,33]

Next, the relaxation rate in the presence of in-plane electric field is discussed. The double dot is assumed to be located in the center of the slab, such that the electron wave function $\varphi(z)$ is even. Since Eq. (13) is an odd function of z, the flexural waves do not contribute to the relaxation rate $(\langle\varphi(z)|\sin(q_{l,n}z)|\varphi(z)\rangle=0)$. Figure 4 reveals an interesting phenomenon. Unlike in bulk systems, the effect of quantized phonon subbands on the relaxation rate is obvious. In most cases, the relevant values are of the order of 10^5-10^7 s^{-1}. In particular, the rate is suppressed $(\Gamma\to 0)$ at a certain electric field (inset). The electron is expected to be able to remain for long time in a quantum state without losses. The divergence of the displacement field $\mathbf{u}(\mathbf{r})$ vanishes at the point such that the function M_n^d plays no role in Eq. (7), importantly indicating that the electron-phonon interaction becomes ineffective.

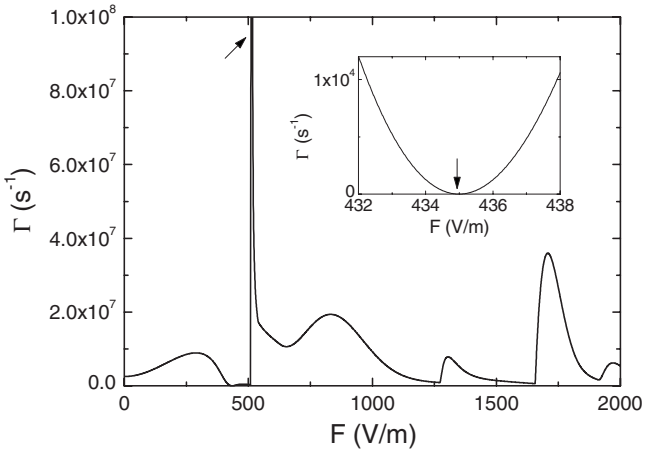

FIG. 4. Relaxation rate Γ as a function of electric field F. The arrow indicates the enhanced relaxation rate. The inset shows a suppressed relaxation rate (arrow). The double dot is located in the center of the slab.

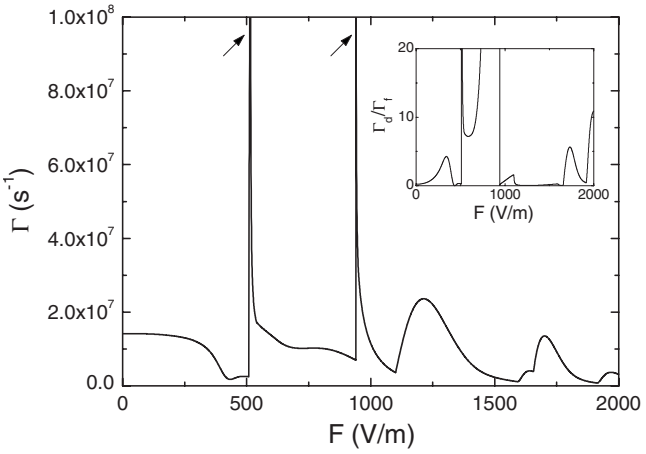

FIG. 6. Relaxation rate Γ as a function of electric field F for fixed position of the double QD (z_0=30 nm). The arrows indicate two enhanced relaxation rates. The inset shows the ratio of the rates for dilatational waves (Γ_d) and flexural waves (Γ_f).

However, Fig. 4 (arrow) displays a dramatically enhanced rate. Figure 3(a) indicates that this fact follows from the van Hove singularity for dilatational waves. Hence, the relaxation rate can be detuned by several orders of magnitude by varying the electric field. Notably, two special features originate from the intrinsic phonon properties of the slab. Analyzing the components of Eq. (7) reveals that the temperature and the vertical width of the QD do not affect the relaxation rates at the points.

Figure 5 plots the specific electric fields in which relaxation rates are enhanced and suppressed with variation in the width of the slab. The electric field plays a flexible role in controlling the energy difference ΔE. The energy difference increases with the field, as shown in the inset.[25] To obtain specific rates, large electric fields are applied when the widths are small. The values drop monotonically as the width increases. The signatures are no longer evident when the slab has large width. In particular, the rate is enhanced only in the large-width regime. This result is explained by the fact that at F=0, the lowest energy difference exceeds the specific phonon energy $\hbar\omega$ for the suppressed or enhanced rate.

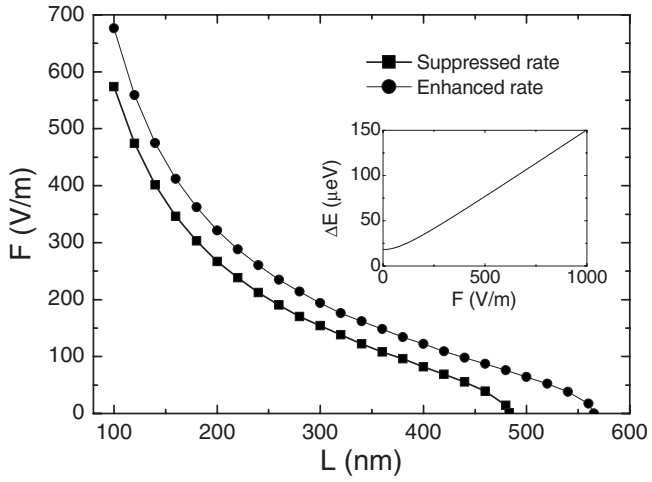

FIG. 5. Dependence of the specific electric field F for the suppressed and enhanced rates on the width of the slab L. The inset shows the energy difference ΔE in the presence of the electric field.

According to the above results, the positions of the dots could be perhaps to influence the relaxation. To demonstrate this point, Fig. 6 plots the relaxation rate versus electric field F for fixed a position of the double QD (z_0=30 nm). Here, z_0 is the displacement of the double QD from the center of the slab. As the dots are not located at the center of the slab, flexural waves start to contribute to the electron relaxation. The total rate consists of two components: dilatational waves and flexural waves. As the electric field increases, the contributions of the two waves complicate the rate. Both components contribute differently to the rate by varying the electric field. As shown in the inset, the main contributor to the relaxation rate changes between the two waves. Figure 6 displays the two enhanced relaxation rates. The important feature is the large asymmetry in the magnitudes of the rates for the two waves. According to Fig. 3, the van Hove singularities are mainly responsible for the obtained rates.

We briefly make some comparison with those used in related studies. Suppression of the relaxation rate is an important issue for researchers who are concerned with the performance of quantum devices. For vertically double QD systems, the relaxation rate is tuned by varying the electric or magnetic field applied in the growth direction.[16–18] Electrons interact with bulk phonons. The modulation of the factor $(\langle f|e^{i\mathbf{q}\cdot\mathbf{r}}|i\rangle)$ enables the relaxation rate to be reduced. On the contrary, in the model employed herein, a lateral double QD is embedded in a suspended slab. An electric field is applied in the interdot direction. A totally different way to control the relaxation rate, which depends on the phonon properties of the slab, is provided. The relaxation rate can be suppressed by tailoring the electron-phonon coupling.

The results for the slab system are compared with those obtained using cavity quantum electrodynamics. In an analogy to the case of confined phonons, the quantized photon modes in the cavity can significantly modify the atomic spontaneous emission. Furthermore, the enhancement or reduction in spontaneous emission is controllable. For example, in a single-mode cavity, the emission decay rate can be increased if the atom is surrounded by a cavity that is

tuned to the transition frequency.[34] Conversely, it decreases when the cavity is detuned.[35] The gaps in the density of states enable spontaneous emission to be completely inhibited in artificial periodic structures.[36,37] This situation is unlike the vanishing of the relaxation rate in the slab that is caused by a real zero in the phonon deformation potential.

IV. CONCLUSIONS

The electron relaxation of lateral double QD systems embedded in suspended slabs is studied. The relaxation rate is strongly modified by the two-dimensional character of the slab phonon. The relaxation rate can be varied by several orders of magnitude by controlling the electric field. Not only can the behavior be enhanced, but also the relaxation rate can be greatly reduced. This flexible mechanism may be useful for quantum devices that are based on lateral double QDs.

ACKNOWLEDGMENTS

This work is supported partially by the National Science Council of Taiwan under the Grant Nos. NSC 97-2112-M-390-006-MY3 and NSC 97-2112-M-009-004.

[1]S. M. Reimann and M. Manninen, Rev. Mod. Phys. **74**, 1283 (2002).
[2]W. G. van der Wiel, S. De Franceschi, J. M. Elzerman, T. Fujisawa, S. Tarucha, and L. P. Kouwenhoven, Rev. Mod. Phys. **75**, 1 (2002).
[3]M. Ciorga, A. S. Sachrajda, P. Hawrylak, C. Gould, P. Zawadzki, S. Jullian, Y. Feng, and Z. Wasilewski, Phys. Rev. B **61**, R16315 (2000).
[4]J. R. Petta, A. C. Johnson, C. M. Marcus, M. P. Hanson, and A. C. Gossard, Phys. Rev. Lett. **93**, 186802 (2004).
[5]O. G. Schmidt, C. Deneke, S. Kiravittaya, R. Songmuang, H. Heidemeyer, Y. Nakamura, R. Zapf-Gottwick, C. Müller, and N. Y. Jin-Phillipp, IEEE J. Sel. Top. Quantum Electron. **8**, 1025 (2002).
[6]R. Songmuang, S. Kiravittaya, and O. S. Schmidt, Appl. Phys. Lett. **82**, 2892 (2003).
[7]Q. Xie, A. Kalburge, P. Chen, and A. Madhukar, IEEE Photonics Technol. Lett. **8**, 965 (1996).
[8]S. Komiyama, O. Astafiev, V. Antonov, T. Kutsuwa, and H. Hirai, Nature (London) **403**, 405 (2000).
[9]I. H. Chan, R. M. Westervelt, K. D. Maranowski, and A. C. Gossard, Appl. Phys. Lett. **80**, 1818 (2002).
[10]D. Loss and D. P. DiVincenzo, Phys. Rev. A **57**, 120 (1998).
[11]T. Hayashi, T. Fujisawa, H. D. Cheong, Y. H. Jeong, and Y. Hirayama, Phys. Rev. Lett. **91**, 226804 (2003).
[12]T. Fujisawa, D. G. Austing, Y. Tokura, Y. Hirayama, and S. Tarucha, Nature (London) **419**, 278 (2002).
[13]U. Bockelmann, Phys. Rev. B **50**, 17271 (1994).
[14]V. N. Stavrou and X. Hu, Phys. Rev. B **72**, 075362 (2005).
[15]H. Y. Ramirez, A. S. Camacho, and L. C. L. Y. Voon, Nanotechnology **17**, 1286 (2006).
[16]G. Q. Hai and S. S. Oliveira, Phys. Rev. B **74**, 193303 (2006).
[17]A. Bertoni, M. Rontani, G. Goldoni, F. Troiani, and E. Molinari, Appl. Phys. Lett. **85**, 4729 (2004).
[18]J. I. Climente, A. Bertoni, G. Goldoni, and E. Molinari, Phys. Rev. B **74**, 035313 (2006).
[19]P. Zhao and D. L. Woolard, Appl. Phys. Lett. **90**, 093507 (2007).
[20]V. N. Stavrou, J. Phys.: Condens. Matter **19**, 186224 (2007).
[21]A. Bertoni, M. Rontani, G. Goldoni, and E. Molinari, Phys. Rev. Lett. **95**, 066806 (2005).
[22]E. M. Höhberger, T. Krämer, W. Wegscheider, and R. H. Blick, Appl. Phys. Lett. **82**, 4160 (2003).
[23]E. M. Höhberger, J. Kirschbaum, R. H. Blick, J. P. Kotthaus, and W. Wegscheider, Physica E (Amsterdam) **18**, 99 (2003).
[24]L. Jacak, A. Wojs, and P. Hawrylak, *Quantum Dots* (Springer, Berlin, 1998).
[25]M. Førre, J. P. Hansen, V. Popsueva, and A. Dubois, Phys. Rev. B **74**, 165304 (2006).
[26]U. Bockelmann and G. Bastard, Phys. Rev. B **42**, 8947 (1990).
[27]B. A. Auld, *Acoustic Fields and Waves* (Wiley, New York, 1973).
[28]N. Bannov, V. Aristov, V. Mitin, and M. A. Stroscio, Phys. Rev. B **51**, 9930 (1995).
[29]H. Bruus, K. Flensberg, and H. Smith, Phys. Rev. B **48**, 11144 (1993).
[30]G. D. Mahan, *Many-Particle Physics* (Plenum, New York, 1990).
[31]S. Vorojtsov, E. R. Mucciolo, and H. U. Baranger, Phys. Rev. B **71**, 205322 (2005).
[32]M. Thorwart, J. Eckel, and E. R. Mucciolo, Phys. Rev. B **72**, 235320 (2005).
[33]S. Debald, T. Brandes, and B. Kramer, Phys. Rev. B **66**, 041301(R) (2002).
[34]E. M. Purcell, Phys. Rev. **69**, 681 (1946).
[35]D. Kleppner, Phys. Rev. Lett. **47**, 233 (1981).
[36]E. Yablonovitch, Phys. Rev. Lett. **58**, 2059 (1987).
[37]S. John, Phys. Rev. Lett. **58**, 2486 (1987).